ANNALS of Faculty Engineering Hunedoara – International Journal of Engineering
Tome XX [2022] | Fascicule 4 [November]

[1.]István ECSEDI, [2.]Dávid GÖNCZI

THERMAL STRESSES IN RADIALLY NON–HOMOGENEOUS CURVED BEAMS

[1,2] Institute of Applied Mechanics, University of Miskolc, Miskolc–Egyetemváros 3515, HUNGARY

Abstract: This paper deals with the determination of displacements and thermal stresses in radially non–homogeneous curved beams which have uniform curvature. The source of the thermal loading is a prescribed steady–state temperature field which depends on the radial coordinate. The developed analytical solution is based on the Euler–Bernoulli beam theory, furthermore the field equations of linear thermoelasticity are used to get the thermal displacements and the stress field. The material properties of the considered curved beam are arbitrary smooth functions of the radial coordinate. Examples of functionally graded materials with exponential and power law based material distributions illustrate the applications of the developed analytical method. The results are compared to results coming from finite element simulations.

Keywords: curved beam, FGM material, steady–state temperature field, thermal stresses

1. INTRODUCTION

Functionally graded materials (FGMs) are advanced materials in which the material composition and hence the material properties vary continuously as a certain function of the spatial coordinate. FGMs have excellent thermomechanical properties and offer great application potential. Recent years a lot of studies have been performed on the mechanics of functionally graded structural components such as [1–6]. Curved beams are frequently used in frame structures, lots of books and papers tackle the stress analysis of such curved beam components e.g. [7–9].

Timoshenko and Goodier [10] found explicit solutions of curved beams under pure bending using the Airy stress function formulation. Lekhnitskii [11] derived the solutions with a specific Young's modulus which was a product of a periodic function of the polar angle and a power law function along the radial coordinate. Bagci [12] studied curved beams and rings of exponentially variable thickness by use of the plane stress state formulation in cylindrical coordinate system. Kilic and Aktas [13] gave a solution of a curved cantilever beam subjected to a single concentrated force at the free end of the beam. Dryden investigated the stresses within a functionally graded curved beam under pure bending condition with a specific function of Young's modulus assuming that, the Poisson's ratio is constant [14].

Paper [15] presented analytical solutions for curved beams of different cross sections under pure bending, where the elastic properties were of a power functions of the thickness coordinate. The paper [16] considered exponential distribution of the material properties within in the curved beam component. Wang and Liu [17] investigated the functionally graded orthotropic elastic beam subjected to uniform loading at its outer surface. In paper [18] analytical solutions are presented for the bending problem of radially graded curved cantilevers on the basis of plane stress formulation. Tufekci et. al. [19] determined the stress and displacement fields in a radially graded beam with arbitrary material distribution in the radial direction under the effect of axial extension and shear deformations with the initial values method. Based on the Euler–Bernoulli beam theory, Pydah and Sabale [20] tackled the flexure problem of bi–directional functionally graded circular beams subjected to various tip loads. The considered curved beam is graded along the radial and tangential directions. Eslami et. al [21] used a two step perturbation technique to present the solution of functionally graded shallow tube subjected to lateral pressure and temperature field, furthermore the properties of the arch were distributed through the radial direction using a power law function. Gao et. al. [22] presented an explicit solution of a curved beam subjected to a concentrated force at the free end of the cantilever beam when the elastic properties vary along the radial direction according to a given power law function. In paper [23] the moduli of elasticity in tension and compression are assumed to be two different exponential functions of the radial coordinate and the stress distributions are determined with power series method. In the work [24] the solution of a radially graded circular curved beam is presented, where the thermal load is obtained from a given temperature field which depends on only the radial coordinate and the modulus of elasticity varies according to a power law function.

In this paper our aim is to give an analytical solution of a curved beam for in plane deformation which is subjected to a given but arbitrary radially nonhomogeneous temperature field. Furthermore, the material properties are arbitrary smooth functions of the radial coordinate.

2. GOVERNING EQUATIONS

Consider a thin circular radially non–homogeneous curved beam of a rectangular cross section (Fig. 1). The curved beam occupies the space domain *B*, whose definition is given by Eq. (1)

$$B=\left\{(r,\varphi,z)\ \middle|\ a\le r\le b,\ -\frac{t}{2}\le z\le\frac{t}{2},\ \varphi_1\le\varphi\le\varphi_2,\ \varphi_1\ne\varphi_2\right\} \tag{1}$$

in the cylindrical coordinate system $Or\varphi z$. The cross section of the curved beam with uniform curvature is shown in Fig. 2. The unit vectors of the cylindrical coordinate system are denoted by $\mathbf{e}_r$, $\mathbf{e}_\varphi$ and $\mathbf{e}_z$. The presented analytical model is based on the Euler–Bernoulli beam theory. The material properties of the considered curved beam depend only on the radial coordinate r, they are smooth functions of the radial coordinate. This type of material inhomogeneity is called radially graded materials [24, 25].

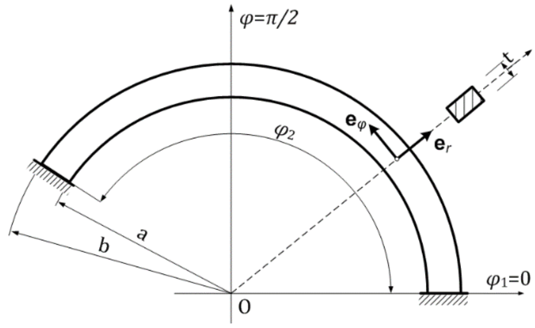

Figure 1. Radially nonhomogeneous curved beam

According to paper [26] the displacement vector $\mathbf{u}$ of the Euler–Bernoulli curved beam in the case of in–plane deformation can be represented as

$$\mathbf{u}=u\mathbf{e}_r+v\mathbf{e}_\varphi+w\mathbf{e}_z,\quad u=U(\varphi),$$
$$v=r\phi(\varphi)+\frac{\mathrm{d}U}{\mathrm{d}\varphi},\quad w=0. \tag{2}$$

Application of the strain–displacement relations of linear elasticity [3, 7, 10] gives

$$\varepsilon_r=\frac{\partial u}{\partial r}=0,\ \varepsilon_z=\frac{\partial w}{\partial z}=0,$$
$$\gamma_{r\varphi}=\frac{1}{r}\frac{\partial u}{\partial\varphi}+\frac{\partial v}{\partial r}-\frac{v}{r}=0, \tag{3}$$

$$\gamma_{rz}=\frac{\partial u}{\partial z}+\frac{\partial w}{\partial r}=0,\ \gamma_{z\varphi}=\frac{1}{r}\frac{\partial w}{\partial\varphi}+\frac{\partial v}{\partial z}=0, \tag{4}$$

$$\varepsilon_\varphi=\frac{1}{r}\left(u+\frac{\mathrm{d}v}{\mathrm{d}\varphi}\right)=\frac{1}{r}\left(\frac{\mathrm{d}^2U}{\mathrm{d}\varphi^2}+U\right)+\frac{\mathrm{d}\phi}{\mathrm{d}\varphi}. \tag{5}$$

In Eqs. (3–5) $\varepsilon_r,\varepsilon_\varphi,\varepsilon_z$ are the normal strains and $\gamma_{r\varphi},\gamma_{\varphi z},\gamma_{rz}$ denote the shearing strains.

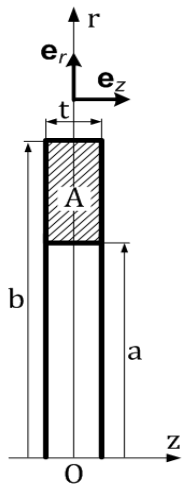

Figure 2. The cross section of the curved beam

The displacement and strain fields given by Eqs. (2–5) satisfy the requirements of the Euler–Bernoulli beam theory [26]. The constitutive law of linear thermoelasticity for the present problem can be formulated as [3, 7, 8, 9]

$$\sigma_\varphi(r,\varphi)=E(r)\left[\varepsilon_\varphi(r,\varphi)-\alpha(r)t(r)\right],$$
$$t(r)=T(r)-T_0. \tag{6}$$

In the previous equation σ_φ denotes the circumferential normal stress, E is the modulus of elasticity, α is the coefficient of linear thermal expansion, T is a given temperature field and T_0 is the reference temperature at which the stresses are zero if the curved beam is loading free. In order to formulate the stress resultant–displacement relations the following cross sectional properties are introduced:

$$AE_0=\int_A E(r)\mathrm{d}A,\quad r_c=\frac{\int_A rE(r)\mathrm{d}A}{EA_0}, \tag{7}$$

$$R=\frac{AE_0}{\int_A r^{-1}E(r)\mathrm{d}A},\quad e=r_c-R. \tag{8}$$

The thermal load is characterized by two quantities in the stress resultant–displacement relations

$$n=\int_A E(r)\alpha(r)t(r)\mathrm{d}A=E_0Ah_n,$$
$$m=\int_A rE(r)\alpha(r)t(r)\mathrm{d}A=E_0Ah_m. \tag{9}$$

The stress resultants are defined according to paper [26] as

$$N(\varphi)=\int_A\sigma_\varphi\mathrm{d}A,\quad M(\varphi)=\int_A r\sigma_\varphi\mathrm{d}A,$$
$$S(\varphi)=\int_A\tau_{r\varphi}\mathrm{d}A, \tag{10}$$

where $\tau_{r\varphi}$ is the shearing stress. In paper [26] the following equilibrium equations are derived:

$$\frac{\mathrm{d}N}{\mathrm{d}\varphi}+S+f_\varphi=0,\quad \frac{\mathrm{d}S}{\mathrm{d}\varphi}-N+f_r=0, \tag{11}$$

$$\frac{\mathrm{d}M}{\mathrm{d}\varphi}+q=0. \tag{12}$$

In Eqs. (11) and (12) $f_r=f_r(r)$ and $f_\varphi=f_\varphi(r)$ are the applied external forces and $q=q(\varphi)$ is the applied moment obtained from the external forces [26]. Combination of Eqs. (6–10) leads to the expressions of $N=N(\varphi)$ and $M=M(\varphi)$

$$N(\varphi)=E_0A\left[\frac{W}{R}+\frac{\mathrm{d}\phi}{\mathrm{d}\varphi}-h_n\right], \tag{13}$$

$$M(\varphi)=E_0A\left[W+r_c\frac{\mathrm{d}\phi}{\mathrm{d}\varphi}-h_m\right], \tag{14}$$

where

$$W(\varphi)=\frac{\mathrm{d}^2U(\varphi)}{\mathrm{d}\varphi^2}+U(\varphi). \tag{15}$$

Assuming that there are no applied external forces, that is

$$f_\varphi=f_r=0,\ q=0. \tag{16}$$

In this case we have

$$S(\varphi)=-\frac{\mathrm{d}N}{\mathrm{d}\varphi}=-E_0A\left[\frac{1}{R}\frac{\mathrm{d}W}{\mathrm{d}\varphi}+\frac{\mathrm{d}^2\phi}{\mathrm{d}\varphi^2}\right]. \tag{17}$$

From Eqs. $(11)_{1,2}$ it follows that

$$\frac{\mathrm{d}^2N}{\mathrm{d}\varphi^2}+N=0. \tag{18}$$

In the presented numerical examples the end cross section at $\varphi=\varphi_1$ is fixed, that is

$$U(\varphi_1)=0,\ V(\varphi_1)=0,\ \phi(\varphi_1)=0,\ (\varphi_1=0), \tag{19}$$

where

$$V(\varphi)=\frac{\mathrm{d}U}{\mathrm{d}\varphi}. \tag{20}$$

From the kinematical boundary conditions it follows that $\mathbf{u}(\varphi_1)=\mathbf{0}$. The reactions at $\varphi=\varphi_1$ are

$$N_0=N(0),\ S_0=S(0),\ M_0=M(0). \tag{21}$$

$B(\varphi)$ denotes the part of the curved beam which is described by Eq. (22)

$$B(\varphi)=\left\{(r,\vartheta,z)\,\middle|\,a\le r\le b,\ z\le\frac{t}{2},\ \varphi_1\le\vartheta\le\varphi\right\}. \tag{22}$$

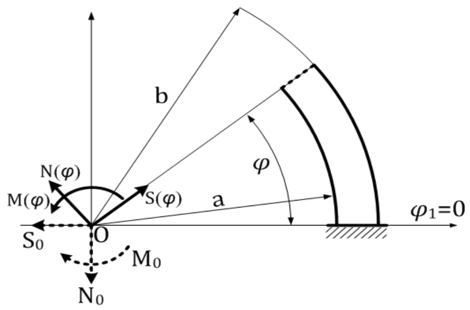

Figure 3. A segment of the curved beam with its mechanical loading

The equilibrium condition of $B(\varphi)$ yields the following results

$$N(\varphi)=N_0\cos\varphi-S_0\sin\varphi,\quad \varphi_1\le\varphi\le\varphi_2, \tag{23}$$

$$S(\varphi)=N_0\sin\varphi-S_0\cos\varphi,\quad \varphi_1\le\varphi\le\varphi_2, \tag{24}$$

$$M(\varphi)=M_0,\quad \varphi_1\le\varphi\le\varphi_2. \tag{25}$$

3. DETERMINATION OF THE THERMAL DISPLACEMENT

Substitution of Eq. (23) into Eq. (13) and substitution of Eq. (24) into Eq. (14) lead to the following coupled system of equations for W and $\frac{\mathrm{d}\phi}{\mathrm{d}\varphi}$:

$$W+R\frac{\mathrm{d}\phi}{\mathrm{d}\varphi}=\frac{N_0R}{AE_0}\cos\varphi-\frac{S_0R}{AE_0}\sin\varphi+Rh_n, \tag{26}$$

$$W+r_c\frac{\mathrm{d}\phi}{\mathrm{d}\varphi}=\frac{M_0}{AE_0}+h_m, \tag{27}$$

From Eqs. (26) and (27) it follows that

$$W(\varphi)=\frac{N_0Rr_c}{AE_0e}\cos\varphi-\frac{S_0Rr_c}{AE_0e}\sin\varphi+\frac{M_0R}{AE_0e}+\frac{Rr_ch_n}{e}-\frac{Rh_m}{e}, \tag{28}$$

$$\frac{\mathrm{d}\phi}{\mathrm{d}\varphi} = -\frac{N_0R}{AE_0e}\cos\varphi + \frac{S_0R}{AE_0e}\sin\varphi + \frac{M_0}{AE_0e} - \frac{Rh_n}{e} + \frac{h_m}{e}. \quad (29)$$

Integration of Eq. (29) with respect to φ between the boundaries $\varphi_1 = 0$ and φ leads to the expression of the cross–sectional rotation

$$\phi(\varphi) = -\frac{N_0R}{AE_0e}\sin\varphi + \frac{S_0R}{AE_0e}(1-\cos\varphi) + \frac{M_0}{AE_0e}\varphi + \frac{h_m - Rh_n}{e}\varphi, \quad \phi(\varphi_1) = 0. \quad (30)$$

Eq. (28) is a second order differential equation for the radial displacement $U = U(\varphi)$:

$$\frac{\mathrm{d}^2U(\varphi)}{\mathrm{d}\varphi^2} + U(\varphi) = \frac{N_0Rr_c}{AE_0e}\cos\varphi + \frac{S_0Rr_c}{AE_0e}\sin\varphi + \frac{M_0R}{AE_0e} + \frac{R}{e}(r_ch_n - h_m). \quad (31)$$

The general solution of differential equation (30) is as follows

$$U(\varphi) = C_1\cos\varphi + C_2\sin\varphi + \frac{R}{e}(r_ch_n - h_m) - \frac{M_0R}{AE_0e} + \frac{N_0Rr_c}{2AE_0e}\varphi\sin\varphi + \frac{S_0Rr_c}{2AE_0e}\varphi\cos\varphi. \quad (32)$$

Substitution of Eq. (31) into Eq. (20) gives

$$V(\varphi) = C_2\cos\varphi - C_1\sin\varphi + \frac{N_0Rr_c}{2AE_0e}(\sin\varphi + \varphi\cos\varphi) + \frac{S_0Rr_c}{2AE_0e}(\cos\varphi - \sin\varphi). \quad (33)$$

The unknown constants C_1 and C_2 and the unknown reactions N_0, S_0, M_0 are obtained from the boundary conditions. In all examples the cross section at $\varphi = \varphi_1$ is fixed, which means that from Eq. (19) we have

$$C_1 - \frac{M_0}{AE_0e} = \frac{R}{e}(h_m - r_ch_n), \quad (34)$$

$$C_2 + \frac{S_0Rr_c}{2AE_0e} = 0. \quad (35)$$

At the end cross section $\varphi = \varphi_2$ three types of boundary conditions will used in the presented numerical examples, which are listed in Table 1.

Table 1. Boundary conditions at the end cross section $\varphi = \varphi_2$

fixed ends	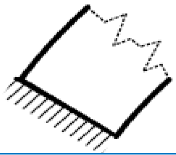	$U(\varphi_2) = 0,\ V(\varphi_2) = 0,$ $\phi(\varphi_2) = 0.$
radially guided end	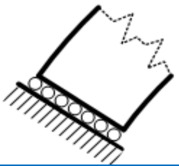	$S(\varphi_2) = 0,\ V(\varphi_2) = 0,$ $\phi(\varphi_2) = 0.$
simply supported in radial direction	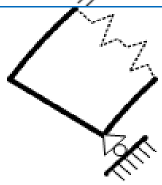	$U(\varphi_2) = 0,\ N(\varphi_2) = 0,$ $M(\varphi_2) = 0.$

4. COMPUTATION OF THE STRESSES

Knowing the displacement field by the use of formula (6) we can get directly the circumferential normal stress σ_φ. The shearing stress $\tau_{r\varphi}$ and normal stress σ_r are obtained from the scalar equations of the equilibrium equation [3, 7, 8, 11]:

$$\frac{\partial\tau_{r\varphi}}{\partial r} + 2\frac{\tau_{r\varphi}}{r} + \frac{1}{r}\frac{\partial\sigma_\varphi}{\partial\varphi} = 0, \quad (36)$$

$$\frac{\partial\sigma_r}{\partial r} + \frac{\sigma_r - \sigma_\varphi}{r} + \frac{1}{r}\frac{\partial\tau_{r\varphi}}{\partial\varphi} = 0. \quad (37)$$

The stresses $\sigma_r = \sigma_r(r,\varphi)$ and $\tau_{r\varphi} = \tau_{r\varphi}(r,\varphi)$ satisfy the following stress boundary conditions on the curved cylindrical boundary surfaces of the beam

$$\tau_{r\varphi}(a,\varphi) = \tau_{r\varphi}(b,\varphi) = 0, \quad \varphi_1 \le \varphi \le \varphi_2, \quad (38)$$

$$\sigma_r(a,\varphi) = \sigma_r(b,\varphi) = 0, \quad \varphi_1 \le \varphi \le \varphi_2. \quad (39)$$

In the present problem the von–Mises stress can be computed as

$$\sigma_M(r,\varphi) = \sqrt{\sigma_r^2 - \sigma_r\sigma_\varphi + \sigma_\varphi^2 + 3\tau_{r\varphi}^2}. \quad (40)$$

5. NUMERICAL EXAMPLES

The next data are valid for all of the presented numerical examples:

$$a = 0.085\mathrm{m},\ b = 0.09\mathrm{m},\ t = 0.5\mathrm{mm}, \quad E_0 = 200\mathrm{GPa}, T_1 = 100\mathrm{K},\ T_2 = 80\mathrm{K}, \quad \varphi_1 = 0,\ t(r) = T_2 + \frac{T_1 - T_2}{b-a}(r-a). \quad (41)$$

Example1. Our first example is a curved beam with fixed cross sections, which is illustrated in Fig. 4.a. The following properties are used in this case:

$$\alpha_0 = 4\cdot 10^{-6}\ \mathrm{K}^{-1},\ \alpha(r) = \alpha_0\left(\frac{r}{a}\right)^2,$$
$$E(r) = E_0\left(\frac{r}{a}\right)^2,\ \varphi_2 = \frac{3\pi}{4}. \qquad (42)$$

The plots of $U(\varphi)$, $V(\varphi)$ and $\phi(\varphi)$ are shown in Figs. (4c–4e).

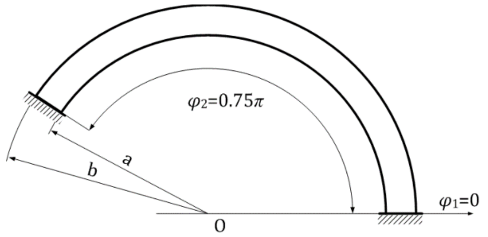

Figure 4.a. Curved beam with fixed ends

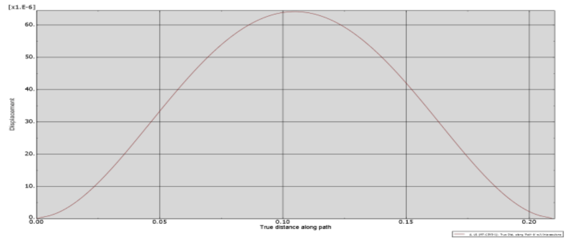
Figure 4b. Radial displacements from FEM solution

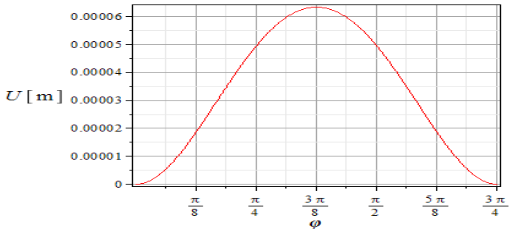

Figure 4c. Radial displacements from analytical solution

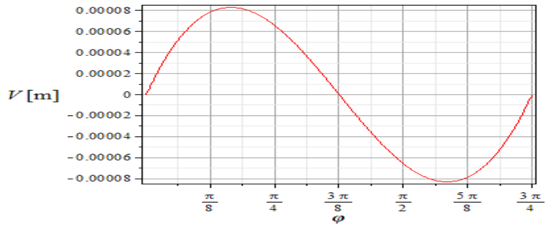

Figure 4d. Plot of $V = V(\varphi)$.

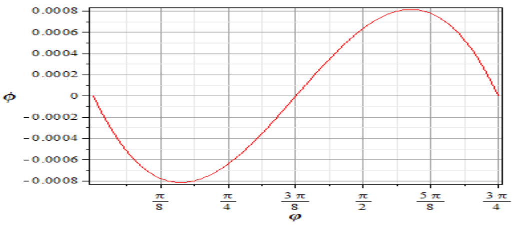

Figure 4e. Plot of $\Phi = \Phi(\varphi)$.

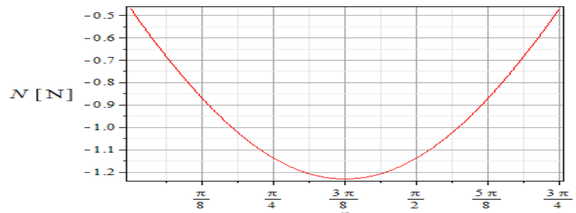

Figure 4f. Plot of $N = N(\varphi)$.

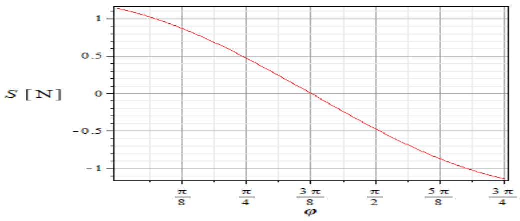

Figure 4g. Plot of $S = S(\varphi)$.

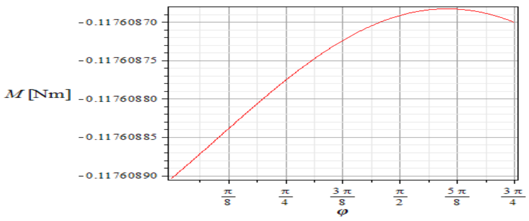

Figure 4h. Plot of $M = M(\varphi)$.

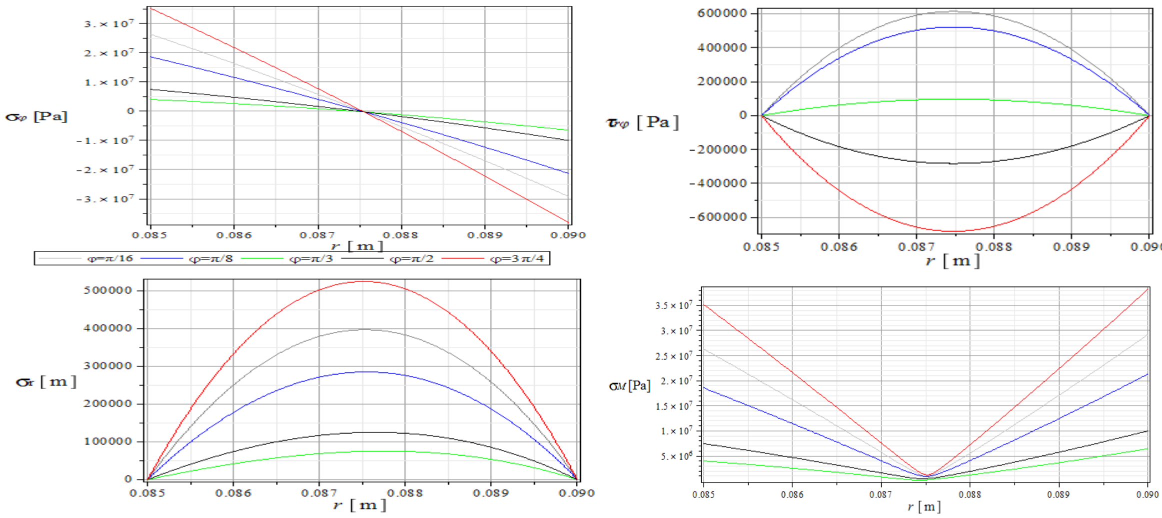

Figure 4j. Plots of stresses

The results are verified by finite element simulations carried out by Abaqus (Fig. 4b). For the finite element modelling of the curved structure quadratic plane stress elements were used in a steady–state coupled temperature–displacement formulation using user defined materials to describe the radially graded material behavior. The solutions coming from the FEA and the developed method are in good agreement.

The graphs of $N(\varphi)$, $S(\varphi)$ and $M(\varphi)$ are presented in Figs. 4f–4h. (The stresses $\sigma_\varphi(r,\varphi)$, $\sigma_r(r,\varphi)$, $\tau_{r\varphi}(r,\varphi)$ and $\sigma_M(r,\varphi)$ as functions of the radial coordinate *r* are shown in Figs. 4j for five different values of φ.

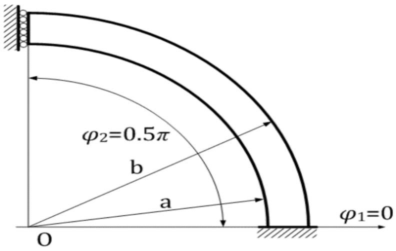

Figure 5a. Curved beam with fixed end and radially guided end

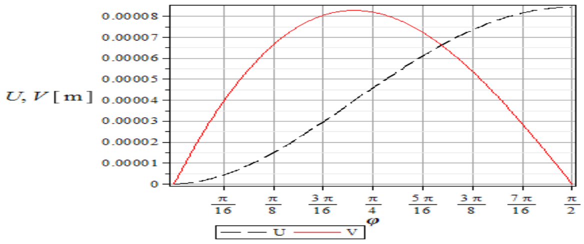

Figure 5b. Plots of the radial displacement function and $V = V(\varphi)$.

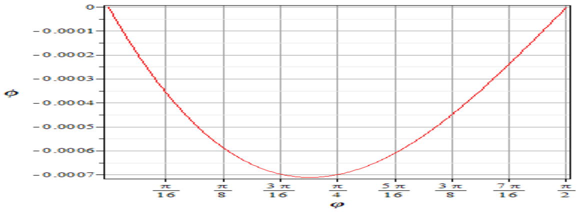

Figure 5c. Plot of $\Phi = \Phi(\varphi)$.

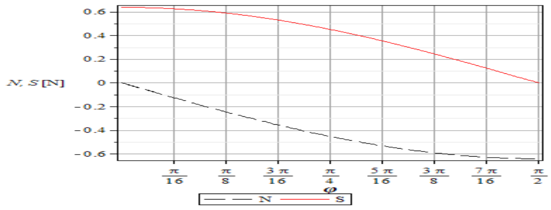

Figure 5d. The graphs of $N = N(\varphi)$ and $S = S(\varphi)$.

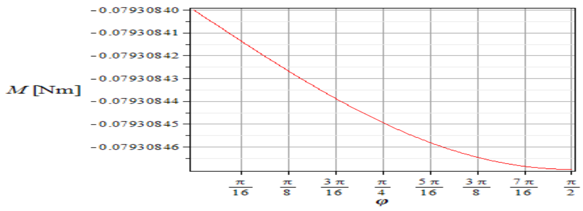

Figure 5e. Plot of $M = M(\varphi)$.

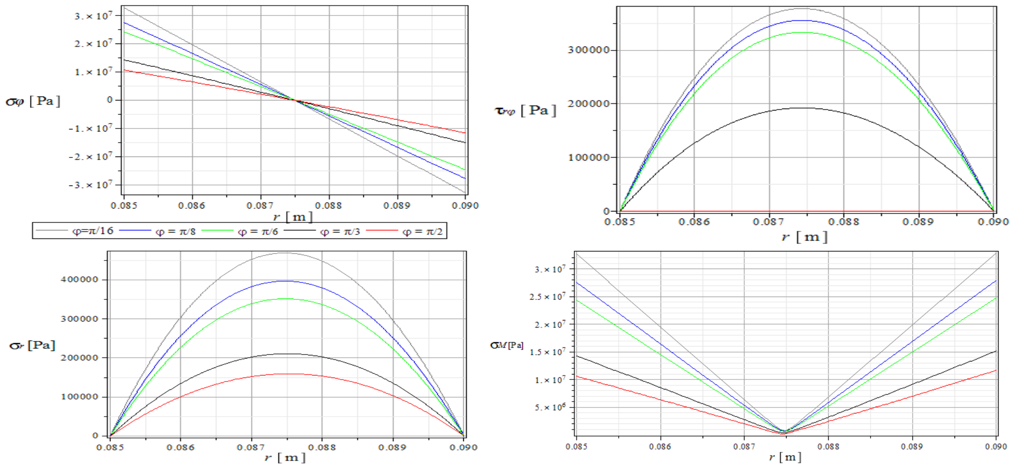

Figure 5f. Plots of stresses

Example2. In the second numerical example a curved beam considered with a fixed and a radially guided end cross sections (Fig. 5a). The following numerical data are used in this example:

$$\alpha_0 = 4\cdot 10^{-6}\,\mathrm{K}^{-1},\ \beta = 1.5(a+b),\ \varphi_2 = \frac{\pi}{2},$$
$$\alpha(r) = \alpha_0 \exp\left(\frac{r}{\beta}\right), E(r) = E_0 \exp\left(\frac{r}{\beta}\right). \tag{43}$$

The plots of $U(\varphi)$, $V(\varphi)$ and $\phi(\varphi)$ are shown in Figs. 5b–5c. The graphs of the inter forces $N(\varphi)$, $S(\varphi)$ and bending moment $M(\varphi)$ are presented in Figs. 5d–5e. The stresses $\sigma_\varphi(r,\varphi)$, $\sigma_r(r,\varphi)$, $\tau_{r\varphi}(r,\varphi)$ and $\sigma_M(r,\varphi)$ as the function of the radial coordinate are shown in Fig. 5f. for five different values of φ.

Example 3. In the third example the curved beam is fixed at one end cross section and simply supported at the other end cross section (Fig. 6a). In this case we have:

$$\alpha_0 = 10^{-4}\,\mathrm{K}^{-1},\ \alpha(r) = \alpha_0\left(\frac{r}{a}\right)^2,$$
$$E(r) = E_0\left(\frac{r}{a}\right)^2,\ \varphi_2 = \pi. \tag{44}$$

Figs. 6b–6d. give the plots of $U=U(\varphi)$, $V=V(\varphi)$, $\Phi(\varphi)$ and Fig.6e illustrates the plots of $N=N(\varphi)$, $S=S(\varphi)$, $M=M(\varphi)$. Figs 6f shows the stresses $\sigma_\varphi(r,\varphi)$, $\sigma_r(r,\varphi)$, $\tau_{r\varphi}(r,\varphi)$ and $\sigma_M(r,\varphi)$ for five different values of φ.

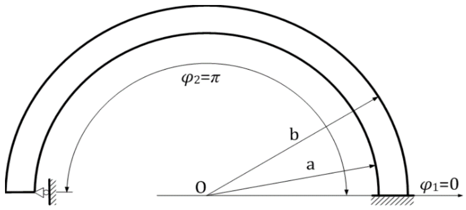

Figure 6a. Curved beam with fixed and simply supported end cross sections

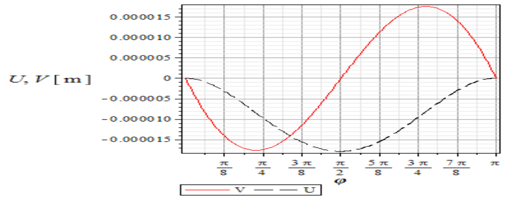

Figure 6b. Plots of $U=U(\varphi)$ and $V=V(\varphi)$ (analytical solution)

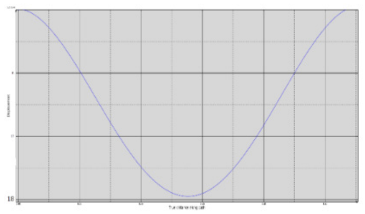
Figure 6c. Plot of $U=U(\varphi)$ (FEM solution).

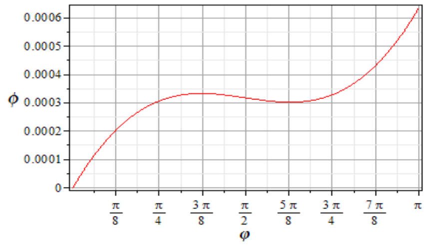

Figure 6d. Plot of $\Phi=\Phi(\varphi)$.

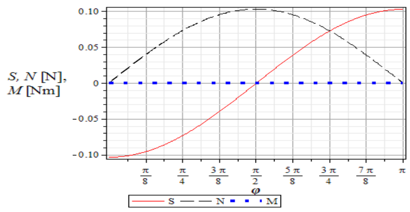

Figure 6e. Plots of $N=N(\varphi)$, $S=S(\varphi)$, $M=M(\varphi)$.

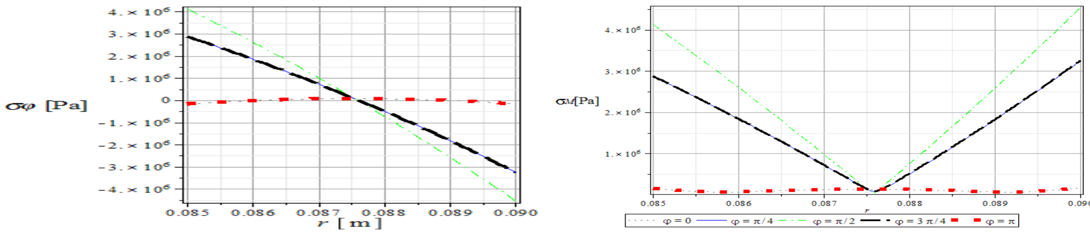

Figure 6f. Plots of the circumferential normal stresses, and von Mises stresses

Example 4. In our last numerical example a radially nonhomogeneous circular ring is considered (Fig. 7a). In this example

$$\alpha_0=10^{-4}\,\mathrm{K}^{-1},\ \alpha(r)=\alpha_0\left(\frac{r}{a}\right)^2. \tag{45}$$

Furthermore the problem is axisymmetric, thus we

$$U(\varphi)=U=\text{constants},\ V(\varphi)=0,\ \phi(\varphi)=0. \tag{46}$$

A simple computation which is based on Eqs. (6, 13, 14, 17) gives

$$U=Rh_n,\ N=0,\ S=0,\ M=E_0A(Rh_n-h_m). \tag{47}$$

In the present problem $U=3.357\cdot10^{-5}$ m, $M=-33.189$ Nmm. The normal stresses $\sigma_r=\sigma_r(r)$, $\sigma_\varphi=\sigma_\varphi(r)$ and von Mises stress $\sigma_M=\sigma_M(r)$ are obtained from Eqs. (48), (49), (50)

$$\sigma_\varphi(r)=E\frac{U(r)}{r}-E(r)\alpha(r)t(r), \tag{48}$$

$$\sigma_r(r)=\frac{U}{r}\int_a^b\frac{E(\rho)}{\rho}\mathrm{d}\rho-\frac{1}{r}\int_a^r E(\rho)\alpha(\rho)t(\rho)\mathrm{d}\rho, \tag{49}$$

$$\sigma_M(r)=\sqrt{\sigma_r^{\,2}-\sigma_r\sigma_\varphi+\sigma_\varphi^{\,2}}, \tag{50}$$

and the graphs of these stresses are shown in Fig. 7b.

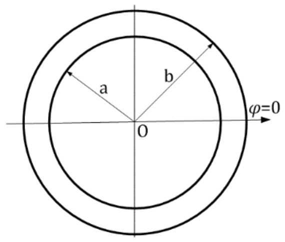

Figure 7a. Radially non–homogeneous circular ring

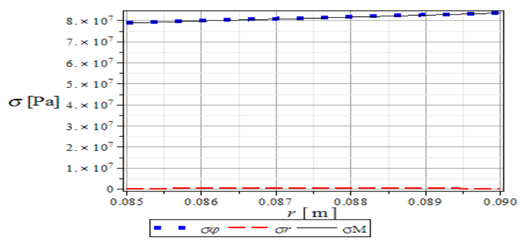

Figure 7b. Plots of stresses

In each example, the results coming from finite element simulations are in good agreement with the analytical solutions, although the accuracy of the FE results significantly depends on the number of elements. To eliminate the oscillation of the results of the commercial FE packages (especially for the stress distribution), sufficiently fine mesh is required.

6. CONCLUSIONS

This paper presents an analytical method for the computation of the stress field and deformations in radially non–homogeneous curved beams and rings. The considered problem is steady state and the developed method is based on the Euler–Bernoulli beam theory, where the applied steady–state thermal field depends only of the radial coordinate. This novel analytical method can be efficiently used to calculate the exact functions for the thermal stresses and displacements within curved beam components made from functionally graded materials and radially layered composites. In these materials the material properties – and the material distribution – are arbitrary functions of the radial coordinate. The developed method can be used as a Benchmark solution for numerical methods. Four examples illustrate the applications of the analytical method, furthermore finite element computations verify the validity of the presented beam formulation.

Acknowledgements

The described article was carried out as part of the EFOP–3.6.1–16–2016–00011 "Younger and Renewing University –Innovative Knowledge City–institutional development of the University of Miskolc aiming at intelligent specialization" project implemented in the framework of the Szechenyi 2020 program. The realization of this project is supported by the European Union, cofinanced by the European Social Fund. This research was (partially) carried out in the framework of Center of Excellence of Innovative Engineering Design and Technologies at the University of Miskolc and supported by the National Research Development and Innovation Office – NKFIH K115701.

References

[1] Pen X, Li X, Thermoelastic analysis of functionally graded annulus with arbitrary gradient. Applied Mathematics and Mechanics (English Edition) 30, 2009, p. 1211–1220
[2] Shi Z, Zhang T, Bending analysis of a piezoelectric curved actuator with a generally graded property for the piezoelectric parameter. Smart Materials and Structures 17 (4), 2008, Article ID 045018
[3] Hetnarsky RB, Eslami MR, Theory of Thermal Stresses. Advanced Theory and Applications, Springer, Berlin, 2010.
[4] Kiss LP, Nonlinear stability analysis of FGM shallow arches under an arbitrary concentrated radial force. International Journal of Mechanics and Materials in Design. 2019
[5] Kiss LP, Free vibrations of rotationally restrained nonhomogeneous circularbeams by means of the Green function. Journal of the Brazilian Society of Mechanical Sciences and Engineering 40:342, 2018
[6] Kiss LP, Sensitivity of FGM shallow arches to the loading imperfection when the loaded by concentrared radial force around the crown. Journal of Non–Linear mechanics 111, 2019, p. 62–72
[7] Nowinski IL, Theory of Thermoelasticity with Applications. Sythoff and Noordhoff, Alpen aan den Rijn, 1978.
[8] Boley BA, Weiner JH, Theory of Thermal Stresses, Dover Publication, New York, 1997.
[9] Carreci E, Fazzolari F, Cinefra M, Thermal Stress Analysis of Composite Beams, Plates, Shells. Academic Press, New York, 2017.
[10] Timoshenko SP, Goodier JN, Theory of Elasticity, McGraw–Hill, New York, USA, 1970.
[11] Lekhnitskii SG, Theory of Elasticity of An Anisotropic Body, Mir Publishers, Moscow, Russia, 1981.
[12] Bagci C, Exact elasticity solutions for stresses and deflections in curved beams and rings of exponential and t–sections. Journal of Mechanical Design 115 (3), 1993, p. 346–358
[13] Kiliç O, Aktaş A, Determination of stress functions of a curved beam subjected to an arbitrarily directed single force at the free end. Mathematical and Computational Applications 7(2), 2002, p. 181–188
[14] Dryden J, Bending of inhomogeneous curved bars. International Journal of Solids and Structures 44 (11–12), 2007, p. 4158–4166
[15] Arefi M, Thermoelastic analysis of functionally graded annulus with arbitrary gradient. Applied Mathematics and Mechanics (English Edition) 30, 2009, p. 1211–1220.
[16] Sankar BV, Tzeng JT, Thermal Stresses in Functionally Graded Beams. AIAA Journal 40 (6), 2002, p. 1228–1232
[17] Wang M, Liu Y, Elasticity solutions for orthotropic functionally graded curved beams. European Journal of Mechanics –A/Solids 37, 2013, p. 8–16
[18] Yu LY, Zhang LL, Bending solution of functionally graded curved–beam. Journal of Engineering Mechanics 31 (12), 2014, p. 4–10
[19] Tufekci E, Eroglu U, Aya SA, Exact solution for in–plane static problems of circular beams made of functionally graded materials. Mechanics Based Design of Structures and Machines 44. (4), 2016, p. 476–494
[20] Pydah A, Sabale A, Static analysis of bi–directional functionally graded curved beams. Composite Structures 160, 2017, p. 867–876
[21] Babaei H, Kiani Y, Eslami MR, Geometrically nonlinear analysis of functionally graded shallow curved tubes in thermal environment. Thin–walled Structured 123, 2018, p. 48–57
[22] Gao Y, Zhang LL, Shang L, Analytical Solutions of Functionally Graded Curved Beams under an Arbitrarily Directed Single Force. Mathematical Problems in Engineering. 4925379, 2019, 11 pages
[23] He X, Li X, Li W, Sun J, Bending analysis of functionally graded curved beams with different properties in tension and compression. Archive of Applied Mechanics 89 (9), 2019, p. 1973–1994
[24] Haskul M, Elastic state of functionally graded curved beam on the plane stress state subject to thermal load. Mechanics Based Design of Structures and Machines 47, 2019
[25] Suresh S, Mortensen A, Fundamentals of Functionally Graded Materials. IOM Communications, New York, 2003.
[26] Ecsedi I, Dluli K, A Linear Model for the Static and Dynamic Analysis of Nonhomogeneous Curved Beams. Applied Mathematical Modelling. 29 (1–2), 2006, p. 1211–1231

ISSN 1584 – 2665 (printed version); ISSN 2601 – 2332 (online); ISSN-L 1584 – 2665